PAPER

Rain Sensing using Dual-Frequency Measurements from Small-Scale Millimeter-Wave Network

Hung V. LE[†*], ***Student Member,*** **Capsoni CARLO**[††], **Nebuloni ROBERTO**[†††], **Luini LORENZO**[††], ***Nonmembers,***
Takuichi HIRANO[†], **Toru TANIGUCHI**[††††], ***Members,*** **Jiro HIROKAWA**[†], ***and*** **Makoto ANDO**[†], ***Fellows***

SUMMARY Dense millimeter-wave networks are a promising candidate for next-generation cellular systems enabling multiple gigabit-per-second data rates. A major disadvantage of millimeter-wave systems is signal disruption by rain, and here we propose a novel method for rain sensing using dual-frequency measurements at 25 and 38 GHz from a small-scale Tokyo Institute of Technology (Tokyo Tech) millimeter-wave network. A real-time algorithm is developed for estimating the rain rate from attenuation using both ITU-R relationships and new coefficients that consider the effects of the rain Drop Size Distribution (DSD). The suggested procedure is tested on measured data, and its performance is evaluated. The results show that the proposed algorithm yields estimates that agree very well with rain gauge data.

key words: *Millimeter-wave Network, Rain Attenuation, Dual-frequency, Rain Sensing, Rain Rate Estimation.*

1. Introduction

In the past few years, the increasing demand for broadband communications has required the use of higher frequencies. Millimeter-waves have received substantial attention because of their high-speed data transmission capabilities and the creation of new frequency resources [1], [2]. In practice, one of the disadvantages of millimeter-wave systems is that these signals can be disrupted by rain. To overcome this difficulty, a dense network consisting of short radio links are proposed in the future wireless systems [3]. Recent reports of global warming effects on weather suggest that the frequency of very intense types of rainfall which are extremely localized (in the order of less than 1 km), is increasing [4], [5]; monitoring the localized rain would be indispensable for the operation of the millimeter-wave networks such as the diversity and also important for reducing potential damages due to heavy rainfalls. In order to monitor the localized rainfalls, dense rain gauge networks are needed [6]. To this end, the rainfall-induced attenuation obtained from the dense millimeter-wave networks could provide an additional and alternative information to the existing rain gauges [7], [8].

Few studies on the estimation of rain rates through commercial telecommunications links have been carried out, Giuli et al. [7] proposed a tomographic technique based on a stochastic approach using the received signal level for estimating the rainfall rate over a specific area with several km long links. In [8], [9], the rain rate was estimated at any given point by using a modified weighted least squares algorithm within a two-dimensional plane using measurements of the received signal level. These conventional studies based on a well-known power law relationship between link signal attenuation and rainfall intensity (ITU-R model) [10], [11] cannot provide the estimation of the heavy rain from the millimeter-wave attenuation correctly, because the ITU-R model is unarguably unsuitable for heavy rainfalls [12], [13]. Moreover, the uncertainties related to Drop Size Distribution (DSD) variations by season, event, or even during a rain event, and their effect on the estimated rain rates are not considered. This is an important issue, as theoretical analysis has shown that the biggest source of error is the variability in the DSD [14]. Recently, in [15] the authors proposed a compressed sensing based detection of localized heavy rain using a microwave network. In [16], Ericsson claimed that microwave links can be used as a local weather radar to save human lives, cut costs to business, and reduce the weather impact on society.

The Microwave Attenuation as a New Tool for the Improving Storm-water Supervision Administration (MANTISSA) project has explored the usage of dual-frequency microwave links to estimate path-integrated rainfall [14]. There, a method using the differences in attenuation along a link at two frequencies is able to recover the frequency-independent DSD variations which give a better estimate of path-averaged rain rates than the one obtained from single frequency measurements. All the above mentioned studies have investigated the macroscopic behavior of rain with relatively long microwave links, and it is difficult to track the localized rainfall due to the DSD variations by season, event, or even during a rain event.

In this paper, an accurate rainfall sensing technique is presented using short links and dual-frequency data at 25 and 38 GHz. Rain attenuation along the path of a link can be obtained as

$$A = \gamma \times d = kR^{\alpha}d \qquad \text{(dB)} \tag{1}$$

where γ (dB/km) is the specific rain attenuation and R

Manuscript received July xx, 2014.
Manuscript revised x xx, 2014.

[†]The authors are with the Graduate School of Science and Engineering, Tokyo Institute of Technology, Tokyo, 152-8552 Japan.
[††]The authors are with Politecnico di Milano, p.zza Leonardo da Vinci 32-20133 Milano, Italy.
[†††]The author is with CNR-IEIIT, Via Ponzio 34/5-20133 Milano, Italy.
[††††]The author is with Japan Radio Co., Ltd., Tokyo, 167-8540 Japan.
[*]Email:vuhung@antenna.ee.titech.ac.jp
DOI: 10.1587/transcom.E0.B.1

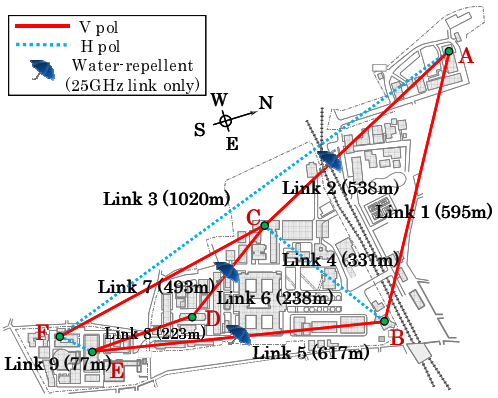

Fig. 1 Tokyo Tech millimeter-wave model network.

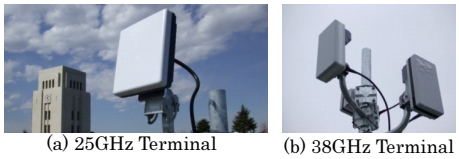

(a) 25GHz Terminal (b) 38GHz Terminal

Fig. 2 Photographs of the wireless terminals.

(mm/h) is the rain rate. The coefficients k and α depend upon the frequency, derived analytically or statistically determined by measurements. Then, the rain rate can be estimated by $R = \left(\frac{A}{kd}\right)^{1/\alpha}$ (mm/h). We have developed a real-time algorithm for estimating the new coefficients k and α respond to the different DSDs by utilizing a frequency scaling technique. The frequency-independent DSD are estimated in the sense of maximizing the likelihood of γ (dB/km) at two frequencies. The frequency-dependent coefficients k and α are derived from this DSD and the relation between the rain rate (R) and specific attenuation (γ) are established. DSD is different for each event and the relation between R and γ also varies with the individual event. In this research, a gamma function DSD model is assumed to select the likelihood of a DSD. The estimation of the rain rate using the coefficients k and α associated with this DSD becomes more accurate based upon dual-frequency measurements at 25 and 38 GHz.

2. Measurement System

2.1 Measurement Installations

The Tokyo Tech millimeter-wave model network consists of 18 Fixed Wireless Access (FWA) links (9 links for 25 GHz and 9 links for 38 GHz), with 6 base stations on the rooftops of as many buildings, as depicted in Fig. 1. The FWA links are connected to each other using network switches at the 6 FWA base stations. The shortest link is 77 m and the longest is 1020 m. Some basic research into millimeter-wave propagation characteristics using this network has been reported in [17]–[20]. Figure 2 shows photographs of the wireless terminals. High gain antennas, about 30 dBi, are used for the FWA terminals which have the specifications listed in Table 1. For the 25 GHz links, a water repellent named HIREC [21] is uniformly coated on the antenna radomes in a thickness of about 15 μm for links 2, 5, and 6.

Table 1 Wireless Terminal Specifications

RF	25 GHz	38GHz
Bandwidth	20 MHz	200 MHz
Duplex scheme	TDD	TDD
Modulation	16QAM	QPSK/16,64QAM
Antenna Gain	29 dBi	32 dBi
Max Trans. Speed	80 Mbps	600 Mbps/1 Gbps

2.2 Dataset

The received signal level (Rx Level) is measured via the received signal strength indicator (RSSI) information, which is calibrated by using pre-measured table relating the IF amplifier output and received signal strength at various temperatures. The bit error rate (BER) is counted as the number of Reed-Solomon error corrections. The Rx level and BER are tentatively stored in the FWA terminal and are monitored by PCs using a simple network management protocol (SNMP) via the Ethernet for the model network. Rainfall intensity is measured by tipping-bucket rain gauges installed at all base stations with 0.2 mm resolution and an average of 1-minute time intervals. The rain rate, Rx Level, and BER were recorded every 5 seconds from 2009 onwards. The rain attenuation is defined as a difference between the average received power of dry and received power of rainy periods. The rain attenuation A is characterized as Eq. (1). In this research, several rainfall events are selected for the analysis to evaluate the proposed technique.

3. Preprocessing

A pre-processing is carried out in order to reduce both the quantization noise of rain attenuation and the effects of radome without the water repellent coating.

3.1 Quantization Noise

When the rainfall intensity is derived from the measured attenuation, it is accompanied by an uneven quantization noise, which strongly depends on the link length and on the attenuation value. For a 1 km link at 25 GHz (attenuation quantization $\Delta A = 0.5$ dB), the rainfall rate uncertainty is

$$\Delta R = \left(\frac{\Delta A}{kd}\right)^{1/\alpha} = \left(\frac{0.5}{k}\right)^{1/\alpha} = 3.2 \quad \text{(mm/h)}, \tag{2}$$

and for the 238 m link, $\Delta R = 15.8$ (mm/h) showing that a short link produces a higher quantization error than a longer link. In 38 GHz wireless terminal, a new A/D converter is introduced and the resolution is higher than that of 25 GHz; $\Delta A = 0.1$ dB and $\Delta R = 0.2$ mm/h and 1.1 mm/h are realized for the long and the short link, respectively. This result suggests that the quantization noise in the estimation

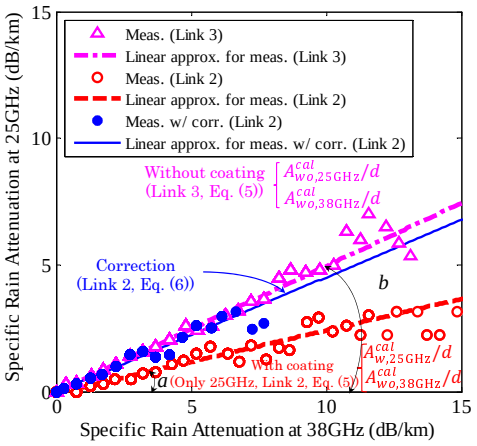

Fig. 3 Frequency scaling of specific rain attenuations (Event on April 28th, 2010). A_w: with repellent coating, A_{wo}: without repellent coating.

of rain rates at high frequencies using short links cannot be neglected. All quantization steps have an equal length, the quantization error is assumed as a uniformly distributed random variable n in the interval $[-1/2\Delta A, 1/2\Delta A]$ as are discussed in [22]. Using $A = kR^{\alpha}d$ and the first-order approximation of the Taylor series, R is approximated by [8], [23] in the final results derived from A,

$$R = R(A+n) \approx \left(\frac{1}{kd}\right)^{1/\alpha} A^{1/\alpha} + \delta \quad \text{(mm/h)}, \tag{3}$$

where an error δ derived from the attenuation measurement and given as

$$\delta = n\left(\frac{1}{kd}\right)^{1/\alpha} \frac{1}{\alpha} A^{\frac{1-\alpha}{\alpha}} \quad \text{(mm/h)}. \tag{4}$$

The quantization error on R is smaller 0.1 mm/h which would be acceptable, allowing the conclusion that approximation (3) gives a better accuracy of the estimated rain rate.

3.2 The Effects of the Radomes and their Calibration

To accurately measure the rain path attenuation along the links, the radome attenuation should be eliminated. The radome attenuation consists of two components, the radome loss due to material loss as well as reflection and the wet radome surface loss due to rain drops layer. The former is canceled by comparing the received signals in dry and rainy weather. In order to estimate the latter, the data for the radome with water repellent coating is referenced. Among nine links with 25 GHz systems, only three links 2, 5, and 6 have antennas with the radomes coated with the HIREC water repellent [21], which are almost free of wet radome surface loss. For all the 25 GHz and 38 GHz links without water repellent coating on radomes, the rain attenuation A_{wo} is calibrated as follows

- We have measured and observed that the radome attenuation during the rain is increasing almost linearly with the rain rate R. The value for $R = 0$ (A_0) has the residual loss of about 1.2 dB at 25 GHz and 1.8 dB at 38 GHz, suggesting 0.6 dB and 0.9 dB loss per antenna, respectively. The value A_0 for radome with water repellent coating is almost zero. All the measured attenuation will be reduced by A_0

$$A^{cal} = A - A_0 \quad \text{(dB)}, \tag{5}$$

where A is the measured attenuation along the links while A_0 represents 0, 1.2 or 1.8 for repellent, for 25 GHz and 38 GHz without the water repellent coating, respectively.
- Figure 3 shows the relations between $A^{cal}_{w\,\text{or}\,wo,25}/d$ for 25 GHz and $A^{cal}_{wo,38}/d$ for 38 GHz measured for two links 2 (in red) and 3 (in pink). $A^{cal}_{w\,\text{or}\,wo,25}/d$ and $A^{cal}_{wo,38}/d$ are proportional with different slopes for Link 2 ($\tan a$) and Link 3 ($\tan b$) in Fig. 3. Since only the antennas of Link 2 at 25 GHz have the water repellent coating, the correction factor for wet radome is derived by $\tan b/\tan a = 1.89$. The attenuation used for the analysis in this paper is derived as follows

$$A^{cal} = (A - A_0)/1.89 \quad \text{(dB)}, \tag{6}$$

- The factor 1.89 approaches to 1 if the link length is very large. In our discussion of small network, the factor 1.89 is assumed to be common for the links with various length and for wide range of rainfall intensity as well as the frequencies. The attenuation data in 38 GHz are also calibrated by (6) as are added by blue in Fig. 3; the measured attenuations for two frequencies with a correction by (6) given in blue are used to establish the best-fit DSD. The procedure is explained in detail in Subsection 4.2. The effectiveness of this calibration (6) should be reviewed later in rain rate estimation.

4. Rain Sensing Technique

4.1 Specific Rain Attenuation

The estimation of rain rates for terrestrial links starts with measuring the specific rain attenuation γ. Here the γ is dependent on the scattering parameters such as the size, shape, and DSD of the rain drops and consequently on the frequency and the polarization. Among these, differences in the DSD that occur during the progress of a rainfall can produce different scaling ratios that depart from the simple scaling relations considered in the ITU-R relation [10], [11]. With heavy rainfalls, this departure occurs at higher attenuation levels, and in order to estimate rain rates accurately, the frequency-dependent coefficients k and α must be computed as a function of the DSD. Frequency-, polarization- and DSD-dependent coefficients k and α required for estimating γ from R along a terrestrial path follow the power-law relationship [10]. The procedure for generating coefficients is as follows

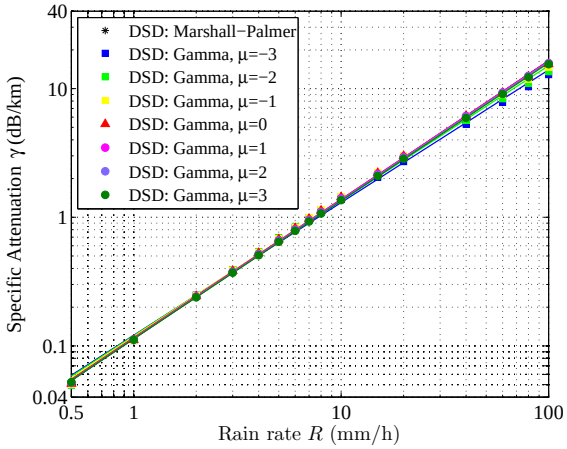

Fig. 4 25 GHz attenuation with H polarization: effect of the DSD.

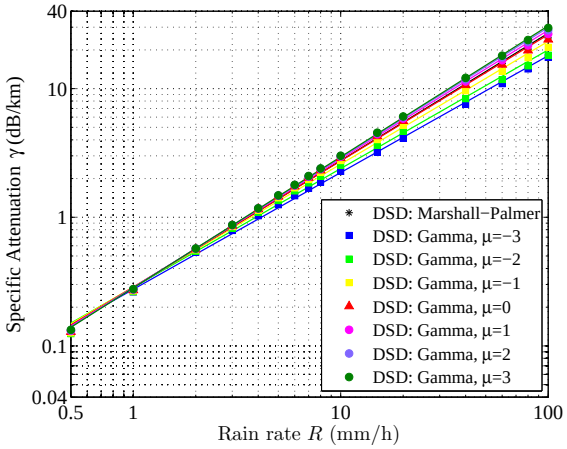

Fig. 5 38 GHz attenuation with H polarization: effect of the DSD.

- Raindrops are modeled as oblate spheroids, and the drops are assumed to descend in stagnant air with the minor semi-axis in the vertical direction (i.e. the canting angle is zero).
- The complex scattering amplitudes $\sigma_{\rm sca}(r)$ have been computed by Holt's program based on the Friedholm integral method (FIM) at the following 19 drop diameters: 0.1, 0.2, 0.3, 0.5, 1.0, 1.5, 2.0, 2.5, 3.0, 3.5, 4.0, 4.5, 5.0, 5.5, 6.0, 6.5, 7, 7.5, and 8.0 mm [24], [25].
- The specific rain attenuation γ associated with several DSDs $n(r)$ is computed according to the well-known single-scattering integral formula as a function of R at different frequencies,

$$\gamma = 4.34 \int_0^\infty \sigma_{\rm ext}(r) n(r) dr \quad ({\rm dB/km}), \tag{7}$$

  where $\sigma_{\rm ext}(r) = \frac{4\pi}{k} \mid {\rm Im}\,[\sigma_{\rm sca}(r)] \mid$ is the extinction cross section of a particle of radius r mm. The DSDs are normalized to satisfy the rain rate integral equation. A generally accepted analytic form of the DSD is the gamma distribution [26],

$$n(r) = N_0 r^\mu e^{-\wedge r} \quad ({\rm mm^{-1}m^{-3}}) \tag{8}$$

$$N_0 = 6 \times 10^{-4} e^{(3.2 - \ln 5)\mu - \ln 5} \quad ({\rm mm^{-1}m^{-1-\mu}}) \tag{9}$$

$$\wedge = 0.2 \left[R / \left(33.31 N_0 5^{\mu+1} \times \right. \right. \tag{10}$$

$$\left. \left. \times \Gamma(4.67 + \mu) \right) \right]^{-1/(4.67+\mu)} \quad ({\rm mm^{-1}}),$$

  where μ is a shape parameter.
- The coefficients k_H, α_H, k_V, and α_V, are obtained by a linear best-fit procedure on log-log axes in the $R - \gamma$ plane for each of the DSDs considered.

The specific rain attenuation γ considering the effect of the DSD at 25 and 38 GHz are shown in Figs. 4, 5, respectively. Higher values of μ cause higher values of rain attenuation for a given rain rate. In [27], it was shown that by categorizing the relationship between any of the DSD parameters $\mu < 0$ is appropriate for orographic rain, which corresponds to a broad DSD curve with a large number of small diameter drops, and $0 < \mu < 2$ may be used for thunderstorm rainfalls, and corresponds to a narrow DSD peak with a small number of small drops. If $\mu = 0$, the DSD takes the form of the standard Marshall-Palmer DSD. For short showers (or very heavy rain), μ is even more variable and no general statement can be made about its range of values. Finally, it must be noted that for a given rain rate R, the γ appears highly dependent on the shape of the DSD: for example, at 100 mm/h, estimates of γ_H at 38 GHz may vary from 18.4 dB/km to about 30.9 dB/km.

Table 2 The k, α coefficients, γ of $R = 100$ mm/h at $f = 25$ GHz

DSD	k_H	α_H	k_V	α_V	γ_H	γ_V
ITU-R 838-3	0.1571	0.9991	0.1540	0.9594	15.6	12.8
Marshall-Palmer	0.1066	1.0865	0.1010	1.0537	15.9	12.9
Gamma, $\mu = -3$	0.1273	1.0172	0.1160	0.9735	13.8	10.3
Gamma, $\mu = -2$	0.1209	1.0428	0.1119	0.9983	14.7	11.1
Gamma, $\mu = -1$	0.1153	1.0657	0.1079	1.0259	15.6	12.2
Gamma, $\mu = 0$	0.1108	1.0801	0.1043	1.0461	16.0	12.9
Gamma, $\mu = 1$	0.1076	1.0852	0.1017	1.0568	15.9	13.2
Gamma, $\mu = 2$	0.1055	1.0844	0.0998	1.0610	15.6	13.2
Gamma, $\mu = 3$	0.1051	1.0797	0.0989	1.0613	15.2	13.1

Table 3 The k, α coefficients, γ of $R = 100$ mm/h at $f = 38$ GHz

DSD	k_H	α_H	k_V	α_V	γ_H	γ_V
ITU-R 838-3	0.4001	0.8816	0.3986	0.8607	23.2	21.0
Marshall-Palmer	0.2826	0.9891	0.2645	0.9747	26.9	23.5
Gamma, $\mu = -3$	0.2891	0.9018	0.2689	0.8817	18.4	15.6
Gamma, $\mu = -2$	0.2941	0.9161	0.2742	0.8960	20.0	17.0
Gamma, $\mu = -1$	0.2935	0.9473	0.2738	0.9299	23.0	19.8
Gamma, $\mu = 0$	0.2893	0.9772	0.2698	0.9627	26.0	22.7
Gamma, $\mu = 1$	0.2849	0.9991	0.2657	0.9867	28.4	25.0
Gamma, $\mu = 2$	0.2811	1.0138	0.2623	1.0030	30.0	26.6
Gamma, $\mu = 3$	0.2756	1.0245	0.2569	1.0149	30.9	27.5

The specific rain attenuation γ (dB/km) is determined as functions of μ and the rain rate R (mm/h) as in Figs. 4 and 5; the fitting of the linear approximation defines the coefficients k and α for a given μ. Tables 2, 3 list the k and α coefficients obtained for the two frequencies here thus far. These coefficients are used as a look-up database to determine the best-fit DSD. Then the measured specific rain attenuation γ_{25} (dB/km) and γ_{38} (dB/km) is compared with the predicted ones in Tables 2 and 3 (the lines in Figs. 4 and 5)

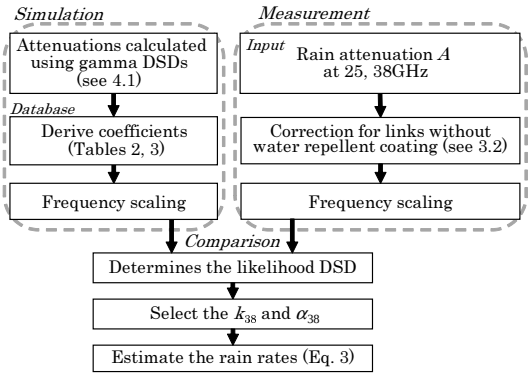

Fig. 6 Flowchart for the real-time algorithm estimating rain rates.

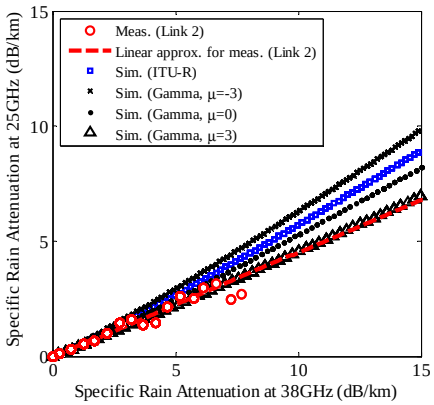

Fig. 7 Frequency scaling of specific rain attenuation with correction for the effects of the antenna radomes (Event on April 28th, 2010).

and so determine the likelihood DSD and μ which minimize the root mean square (RMS) errors. The procedure is fast and could be used as a real-time algorithm for estimating rain rates as explained in the next subsection.

4.2 Rain Rate Estimation

Figure 6 shows a flowchart of the proposed real-time algorithm for estimating rain rates using the measured rain attenuation. The frequency scaling technique is used to determine the likelihood coefficients k and α. The procedure can be summarized below for the moderate rain as an example.

- The measured specific rain attenuations γ after correction for the effects of the antenna radomes are used to plot the frequency scaling as shown in Fig. 7.
- In the simulations, the coefficients k and α are determined from a look-up database as in Tables 2 and 3 for a given DSD at 25 and 38 GHz. The simulated frequency scaling are also plotted in the same figure for typical values of DSDs.
- At each time-step, the algorithm determines the likelihood of a DSD for the two frequencies considering the RMS errors between the simulation and measured frequency scaling,

$$\text{RMS} = \sqrt{\frac{1}{2M} \parallel \text{vec}\{\gamma\} - \text{vec}\{\tilde{\gamma}\} \parallel_F^2}, \qquad (11)$$

where $\gamma = [\gamma_{38}, \gamma_{25}]$, $\tilde{\gamma} = [\tilde{\gamma}_{38}, \tilde{\gamma}_{25}]$ are measured and simulated specific attenuation at 38 and 25 GHz. For example, Fig. 7 plots the simulation with ITU-R, gamma DSDs of $\mu = -3, 0$, and 3 together with the measured frequency scaling results. In this rainfall event, the best-fit DSD is a gamma DSD of $\mu = 3$.

- Then, the coefficients k and α associated with this DSD are used for estimating the rain rates using Eq. (3).

A software program has been developed for the practical implementation using the rainfall estimation technique, as demonstrated in the next section. We calculate the rainfall progressively accumulated during the rain event, as the parameter which is useful in rain disaster monitoring. The accumulated rain $\bar{R}$ (mm) was calculated as follows,

$$\bar{R} = \int_0^T R_i dt \approx \sum_{i=0}^{T} R_i \Delta T \quad \text{(mm)}, \qquad (12)$$

where R_i is the rain rate at time i, ΔT is the time resolution. Cumulative differences are also introduced to know the difference in percentage between the values estimated by the proposed method, the ITU-R values, and the rain gauge data. The cumulative difference is defined as follows

$$\%\text{Difference} = \frac{\sum_{i=0}^{T} \mid R_i - \tilde{R}_i \mid \Delta T}{\bar{R}} \times 100\%, \qquad (13)$$

where R_i and $\tilde{R}_i$ are the measured and estimated rain rates at time i.

5. Results

To demonstrate the effectiveness of the proposed method for determining rainfall rates, three rainfall events were selected for the analysis:

- Event 1: Weak rainfall event (peak averaged rain rate $R_p = 6.3$ mm/h) on March 25th, 2010.
- Event 2: Moderate rainfall ($R_p = 25.8$ mm/h) event on April 28th, 2010.
- Event 3: Heavy rainfall ($R_p = 180$ mm/h) event on July 23rd, 2013.

5.1 Event 1 (Weak rainfall event)

Figure 8 shows the specific rain attenuations obtained from the attenuation measurements collected for Link 3 (1020m) at 25 and 38 GHz during the Event 1 (weak rainfall event). Here the attenuation at 38 GHz is larger than that of 25 GHz, and the attenuation at 38 GHz is used to estimate the rain rate in this rainfall event. The proposed algorithm searches the most likely DSD for each rain event. The best-fit coefficients k and α for this specific event are the coefficients proposed by ITU-R assuming Laws-Parsons DSD rather than Gamma DSD. So, μ, the parameter of Gamma DSD, was

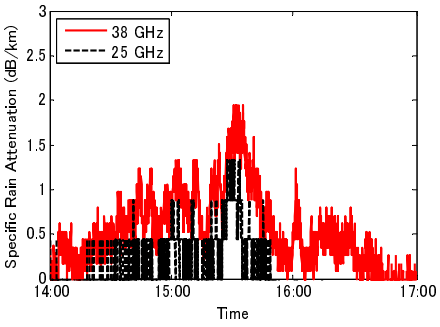

Fig. 8 Specific rain attenuation at 25 and 38 GHz (Event 1).

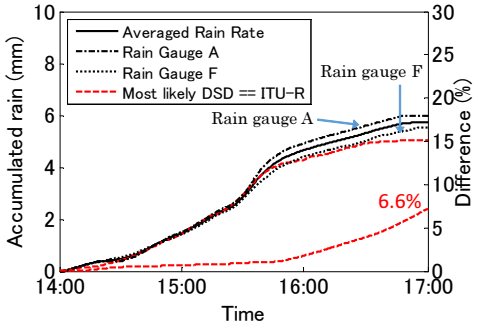

Fig. 11 Accumulated rain using estimates from Link 3 (Event 1).

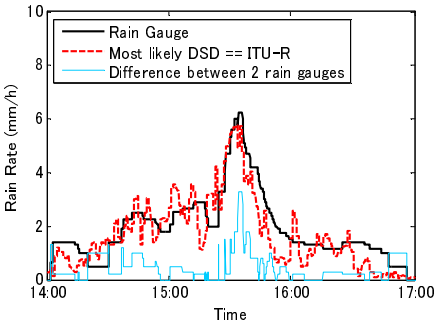

Fig. 9 Estimated rain using the attenuation of Link 3 at 38 GHz. The most likely coefficients are ITU-R coefficients (Event 1).

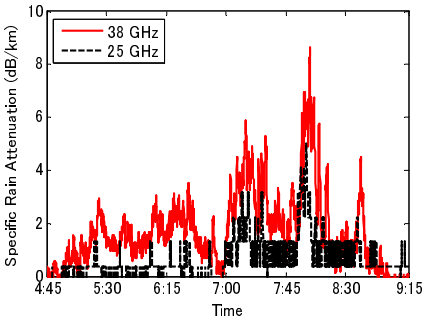

Fig. 12 Specific rain attenuation at 25 and 38 GHz (Event 2).

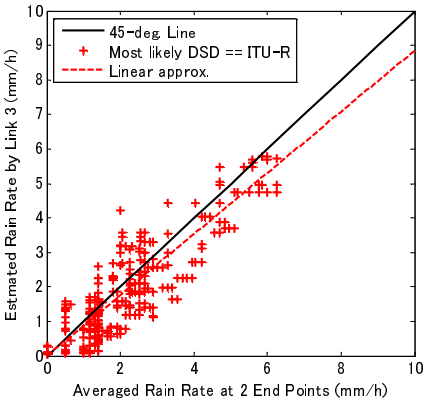

Fig. 10 Estimated rain using the attenuation of Link 3 at 38 GHz (Event 1).

not derived. Figures 9 and 10 show the estimated rain rate using the rain attenuation of Link 3 with ITU-R coefficients. These results indicate that the estimated rain rates using ITU-R coefficients are in good agreement with the averaged rain rate at the two end points (A and F) of the link, which is represented by the 45-deg linear line in Fig.10. Normally, in the weak rainfall events, there are many small raindrops in spherical shape. And it is appropriate to apply the ITU-R model based on the Laws-Parsons DSD, in which raindrops are modeled as spherical shape. The results suggest that the ITU-R coefficients can be directly used for estimating weak rain rates. There is some variation in the rain rates due to quantization errors which are not negligible with respect to such small rain rates, but these are within the acceptable range. The difference in the rain rates between the two rain gauges is also plotted in Fig. 9, suggesting localized variations in the rainfall even for the short link with the length 1 km.

Figure 11 shows the average rainfall progressively accumulated during the rain event (same data as in Figs. 9 and 10) which is important for disaster warnings; the results largely agree within an overall percentage difference of 6.6% after the 3-hour period of the event. The accumulated rainfalls obtained from the two rain gauges A and F are plotted in the same figure. It is observed that localized phenomena of the rain slightly increases deviation of these from that of averaged one in the accumulated rainfall.

5.2 Event 2 (Moderate rainfall event)

For the moderate rain event, Fig. 12 shows the rain attenuation values obtained from the attenuation collected by Link 2 (538m) at 25 and 38 GHz. Figures 13 and 14 show the estimated rain rates compared with the averaged rain rates measured at the two end points (A and C) of Link 2 at 38 GHz. The most likely DSD for this event is a gamma DSD of $\mu = 3$. For comparison, the estimated rain rate using the ITU-R coefficients is also plotted, in blue (Figs. 13, 14). During the light rain here, lower than 10 mm/h for example, the estimated rain rates using the proposed method are very

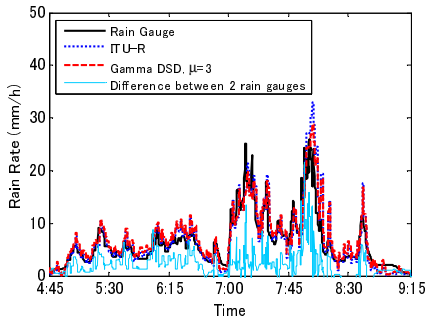

Fig. 13 Estimated rain using the attenuation of Link 2 at 38 GHz (Event 2).

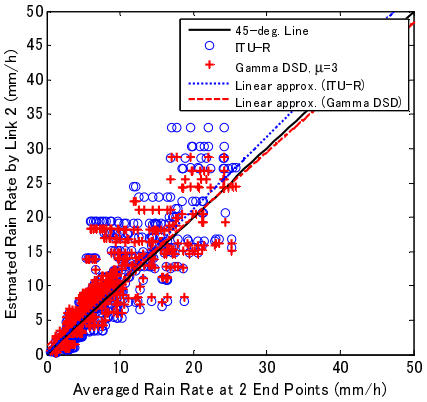

Fig. 14 Estimated rain using the attenuation of Link 2 at 38 GHz (Event 2).

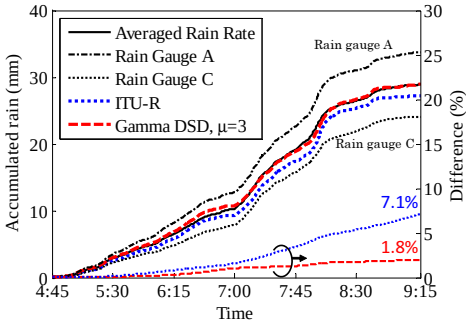

Fig. 15 Accumulated rain using estimates from Link 2 (Event 2).

similar to those using the ITU-R coefficients. However, at the higher precipitation rates ($R > 10$ mm/h), the estimated rain rates from the dual-frequency measurements are superior to those obtained using the ITU-R coefficients. The results suggest that variations in the DSD are more significant at higher rain rates.

In Fig. 15, the accumulated rainfall is plotted using the Fig. 14 data with the relative difference over the whole 4.5 hour period around 1.8% with the proposed method, versus 7.1% using the ITU-R coefficients. It is also observed that locality of rain rapidly increases with the rain rate and

Fig. 16 A photo of the rainfall event on July 23rd, 2013 at Odaiba, Tokyo.

accounts for increasing differences in rain accumulation between two rain gauges. This result suggests the local features of the moderate rainfalls. The rain accumulation estimated from the radio links stays close to the averaged one and suggests the reasonable alternative data.

5.3 Event 3 (Heavy rainfall event)

To evaluate the effectiveness of the proposed method with intense precipitation, Event 3 noted above, was selected for the analysis. Figure 16 shows a photo of this heavy rainfall event on July 23rd, 2013 at Odaiba, Tokyo [28]. Figure 17 shows the rainfall maps at 3 time points (15:30-16:30), extracted from the report of the Tokyo District Meteorological Observatory [29]. The speed of the progress of the storm was very high at about 40 km/h, and extremely high rain intensities were recorded. The peak rainfall rate recorded at Tokyo Tech was about 180 mm/h. During this downpour, the water level of Meguro River rose above the danger water level, and Tokyo Metropolitan Railway and Tokaido Shinkansen services were suspended due to the heavy rains and lightning strikes. These emergency conditions show the need for monitoring heavy rain events like this to reduce damage.

Figure 18 shows the specific rain attenuations obtained from the attenuation of Link 8 (223m) at 25 and 38 GHz for Event 3. To evaluate the effects of the rainfall intensity and of the variation in the DSD on the estimates of large rain rates using the proposed method, the rain attenuations are grouped into: $0 < \gamma \leq 3$ (dB/km), $3 < \gamma \leq 12$ (dB/km), $12 < \gamma \leq 20$ (dB/km), and $20 \leq \gamma$ (dB/km), corresponding to “slight”, “moderate”, “heavy”, and “violent” rainfalls as shown in Fig. 18. ITU-R, Gamma DSDs of $\mu = -3, -2$, and -3 in turn are the most likely DSDs for the above four groups of specific rain attenuations. It is noted that the DSD for the range $3 < \gamma \leq 12$ ($\mu = -3$) is different from Event 2 ($\mu = 3$) with the γ in almost the similar range $0 < \gamma \leq 10$ (dB/km).

Figures 19 and 20 show the estimated rain rates compared with the rain rate actually observed with rain gauge D. Since the link length is short, only one rain gauge is used in the discussion here. There is reasonable agreement between the estimated rain rate and the actual measurements. The results were also compared with what was obtained using the ITU-R coefficients (in blue): the results show that the estimated rain rates are satisfactory only for the weak rainfall rates; however, at the higher rain rates, the accuracy of the

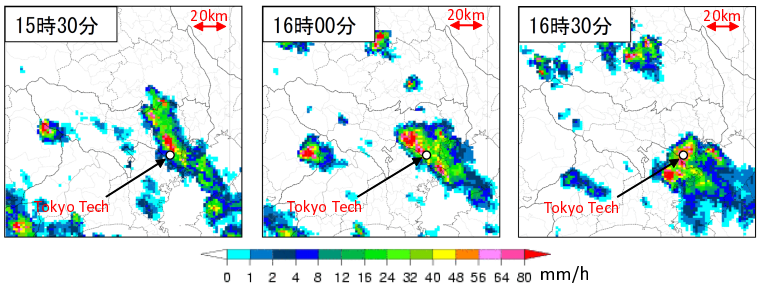

Fig. 17 Rainfall maps at 3 time slots (15:30-16:30) in the Tokyo area on July 23rd, 2013.

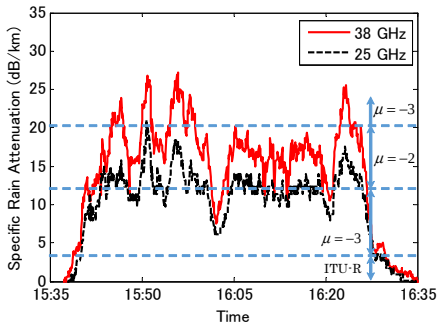

Fig. 18 Specific rain attenuation at 25 and 38 GHz (Event 3).

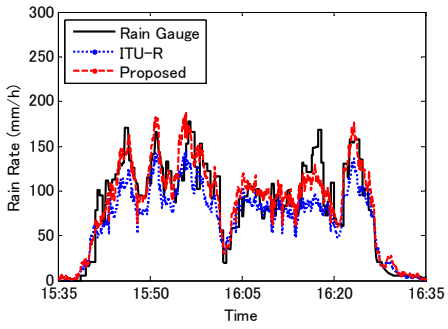

Fig. 19 Estimated rain using the attenuation of Link 8 at 38 GHz (Event 3).

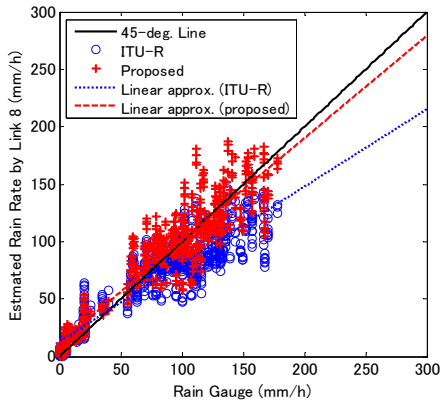

Fig. 20 Estimated rain using the attenuation of Link 8 at 38 GHz (Event 3).

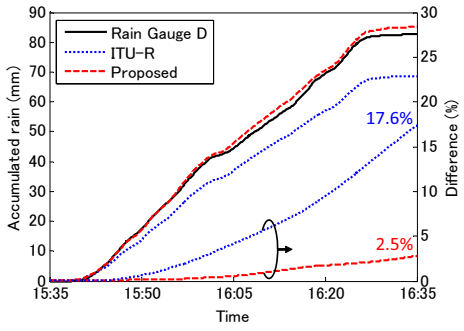

Fig. 21 Accumulated rain using estimates from Link 8 (Event 3).

ITU-R coefficients is poorer.

Figure 21 shows the accumulated rain amount using the Fig. 20 data, the results indicate that the estimated accumulated rain agrees with the rain gauge data within a difference of 2.5% over the whole of the 1-hour period. Using the ITU-R coefficients, this difference is as much as 17.6% over the same period, clearly showing that incorporating the variability of the DSD improves the rain rate prediction accuracy. This result provides a more accurate performance in estimating rain rates using the dual-frequency links by taking into account the variation in the DSD during rain events (which is achieved by defining specific rain attenuation classes). These results suggest that weak, moderate rainfall events do not need the categorization and that one DSD is enough except in the case of heavy rainfalls, and certainly that it is advisable to use different DSDs for each category.

6. Conclusion

In this paper, a deterministic algorithm was presented for observing rainfall intensities. Frequency-dependent coefficients to estimate specific rain attenuations were derived. An estimation technique of rain rates considering the effects of DSDs characterized by a complex variable μ was proposed, which reflects DSD and varies dynamically for the strong rain. The rain rate estimation method was verified with data from short range terrestrial links and variety of

rain rate including a very heavy rain event in Tokyo. The rain rate estimation by the proposed method, which takes into account the effects of DSDs, shows an enhanced agreement to that by rain gauges' data especially for heavy rain. Now, the rainfall-induced attenuation could provide a real-time rain rate monitoring alternative to the rain gauges, for wide variety of heavy rainfalls.

In the future, an algorithm for early prediction of rainfall rates from past data will be proposed.

Acknowledgment

This work was conducted in part as "the Research and Development for Expansion of Radio Wave Resources" under the contract of the Ministry of Internal Affairs and Communications.

References

[1] J. A. Wells, "Faster than fiber: the future of multi-Gb/s wireless," IEEE Microwave Mag., vol. 10, no. 3, pp. 104-112, 2009.
[2] Z. Pi and F. Khan, "An introduction to millimeter-wave mobile broadband systems," IEEE Commun. Mag., vol. 49, no. 6, pp. 101-107, Jun. 2011.
[3] K. Sakaguchi et. al., "Millimeter-wave evolution for 5G cellular networks," IEICE Trans. Commun., vol. E98-B, no. 3., Mar. 2015.
[4] J. Joel, B. Alexis, "Quantification of the small-scale spatial structure of the raindrop size distribution from a network of disdrometers," J. Appl. Meteor. Climatol., vol. 51, pp. 941-953, 2012.
[5] L. Pedersen et. al., "Quantification of the spatial variability of rainfall based on a dense network of rain gauges," Atmospheric Research, vol. 95, pp. 441-454, 2010.
[6] K. Hiroi et al., "Accurate and early detection of Localized Heavy Rain by integrating multivendor sensors in various installation environments," IEEE SENSORS, Maryland, USA, Nov. 2013.
[7] D. Giuli et al., "Microwave tomographic inversion technique based on stochastic approach for rainfall fields monitoring," IEEE Trans. Geos. and Remote Sens., vol. 37, no. 5, pp. 2536-2555, Sept. 1999.
[8] O. Goldshtein et al., "Rain rate estimation using measurements from commercial telecommunication links," IEEE Trans. Signal Process., vol. 57, no. 4, pp. 1616-1625, Apr. 2009.
[9] D. Cherkassky et al., "Precipitation classification using Measurements from commercial microwave links," IEEE Trans. Geos. and Remote Sens., vol. 52, no. 5, pp. 2350-2356, May 2014.
[10] R. Olsen et al., "The aR^b relation of rain attenuation," IEEE Trans. Antennas Propag., vol. AP-26, pp. 318-328, Mar 1978.
[11] Rec. ITU-R. P.838-3, "Specific attenuation model for rain for use in predictions methods," ITU-R Recommendations and Reports, ITU, Mar. 2005.
[12] A. Y. Abdulrahman et al., "A new rain attenuation conversion technique for tropical regions," Progress In Electromagnetics Research B, Vol. 26, pp. 53-67, 2010.
[13] M. R. Islam and A. R. Tharek, "Propagation study of microwave signals based on rain attenuation data at 26 GHz and 38 GHz measured in Malaysia," in Proceedings IEEE Asia Pacific Microwave Conference (APMC 1999), Singapore, Dec. 1999.
[14] M. D' Amico et al., "The MANTISSA project: First results from the Italian field experiments," in Proc.IEEE Int. Geosci. Remote Sens. Symp. (IGARSS'03), 2003, pp. 4314-4316.
[15] G. D. Abrajano and M. Okada, "Compressed sensing based detection of localized heavy rain using microwave network attenuation," The 7th European Conference on Antennas and Propagation (EuCAP 2013), Gothenburg, Sweden, Apr. 2013.
[16] Ericsson, "Micro weather," Mobile World Congress (MWC2014), Barcelona, Feb. 2014.
[17] T. Hirano et al., "Estimation of rain rate using measured rain attenuation in the Tokyo Tech millimeter-wave model network," IEEE AP-S International Symposium, Toronto, Canada, June 2010.
[18] H. V. Le et al., "Quantitative Analysis of Rainfall Variability in Tokyo Tech MMW Small-Scale Model Network," 2013 International Symposium on Antennas and Propagation (ISAP 2013), Nanjing, China, Oct. 2013.
[19] H. V. Le et al., "Link correlation property in Tokyo Tech millimeter-wave model network," 2013 IEEE International Symposium on Antennas and Propagation (AP-S 2013), Florida, USA, Jul. 2013.
[20] H. V. Le et al., "Millimeter-wave propagation characteristics and localized rain effects in a small-scale university campus network in Tokyo," IEICE Trans. Commun., vol. E97-B, no. 5, pp. 1012-1021, May 2014.
[21] HIREC: http://www.ntt-at.com/product/hirec/
[22] B. Widrow, and I. Koll'ar, "Quantization noise: roundoff error in digital computation, signal processing, control, and communications," Cambridge University Press, Cambridge, UK, 2008.
[23] A. Zinevich et al., "Prediction of rainfall intensity measurement errors using commercial microwave communication links," Atmos. Measure. Tech., vol. 3, pp. 1385-1402, 2010.
[24] M. Thurai, and V. N. Bringi, "Drop axis ratios from 2D video disdrometer," J. Atmos. Oceanic Technol, vol. 22, pp. 966-978, 2005.
[25] N .K. Uzunoglu et al., "Scattering of electromagnetic radiation by precipitation particles and propagation characteristics of terrestrial and space communication systems," Proceedings of the Institution of Electrical Engineers, vol. 124, No.5, pp.417-424, 1977.
[26] R. Nebuloni, C. Capsoni, "Effect of hydrometeor scattering on optical wave propagation through the atmosphere," The Fifth European Conference on Antennas and Propagation (EuCAP 2011), Rome, Italy, Apr. 2011.
[27] C. W. Ulbrich, "Natural variations in the analytical form of the raindrop size distribution," J. Climate Appl. Meteor., vol. 22, pp. 1764-1775, 1983.
[28] ANN News on Jul. 23, 2013.
[29] Tokyo District Meteorological Observatory, "Preliminary report of heavy rainfall event on Mar. 23, 2013,"

Hung V. Le was born in Vietnam, in 1984. He received the B.E. degree from The University of Electro-Communications, Tokyo, Japan, in 2010 and the M.E. degree from Tokyo Institute of Technology, Tokyo, Japan in 2012, where he is working toward the Ph.D. degree. In 2014, he was a visiting Ph.D. student at Politecnico di Milano. His current research interests are propagation prediction modeling in wireless communication systems and millimeter wave propagation. Mr. Le is a student member of the IEEE.

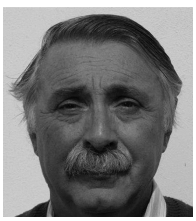

Carlo Capsoni graduated in electronic engineering at the Politecnico di Milano, Milan, Italy, in 1970. In 1970, he joined the "Centro di Studi per le Telecomunicazioni Spaziali" (CSTS) at the Politecnico di Milano. In this position he was in charge of the installation of the meteorological radar of the CNR sited at Spino d'Adda, Italy, and since then he is the scientific responsible for the radar activity. In 1979, he was actively involved in the satellite Sirio SHF propagation experiment (11-18 GHz) and later in the Olympus (12, 20 and 30 GHz) and Italsat (20,40 and 50 GHz) satel-

lites experiments. His scientific activity is mainly concerned with theoretical and experimental aspects of electromagnetic wave propagation at centimeter and millimeter wavelengths in presence of atmospheric precipitation with particular emphasis on attenuation, wave depolarization, incoherent radiation, interference due to hydrometeor scatter, precipitation fade countermeasures, modeling of the radio channel and design of advanced satellite communication systems. The scientific activity in the field of radar meteorology is mainly focused on rain cell modeling for propagation applications, on the development of radar simulators and on the study of the precipitation microphysics. In 1986 he became Full Professor of electromagnetics at the same University. He was member of the ITU national group and was the Italian delegate in COST projects (COST 205, 210).

Roberto Nebuloni received the Laurea degree in Electronic Engineering and the PhD degree in Information Engineering from the Politecnico di Milano, Milan, Italy, in 1997 and 2004, respectively. In December 2005, he joined the Italian National Research Council, Milan, where he is currently a Researcher in the Istituto di Elettronica e Ingegneria Informatica e delle Telecomunicazioni. His research interests include millimeter and optical-wave propagation and radar applications in the fields of telecommunications and meteorology.

Lorenzo Luini was born in Italy, in 1979. He received the Laurea Degree in telecommunication engineering in 2004 and the Ph.D. degree in information technology in 2009 both from Politecnico di Milano, Milan, Italy. He is currently an Assistant Professor at DEIB (Dipartimento di Elettronica, Informazione e Bioingegneria). Since 2004, his research activities have been relative to E.M. wave propagation through the atmosphere, both at radio and optical frequencies: physical modeling and synthesis of the meteorological environment; development and implementation of models for the remote sensing of atmospheric constituents using radiometric data; physical and statistical modeling for E.M. propagation applications. He has been involved in several European COST projects, in the European Satellite Network of Excellence (SatNEx), as well as in several projects commissioned to the research group by the European Space Agency (ESA) and the USA Air Force Laboratory.

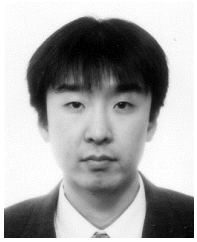

Takuchi Hirano was born in Tokyo, Japan, on January 28, 1976. He received the B.S. degree in electrical and information engineering from the Nagoya Institute of Technology, Nagoya, Japan, in 1998, and the M.S. and D.E. degrees from the Tokyo Institute of Technology, Tokyo, Japan, in 2000 and 2008, respectively. He is currently an Assistant Professor with the Tokyo Institute of Technology. He has been involved with EM theory, numerical analysis of EM problems, and antenna engineering including slotted waveguide arrays. Dr. Hirano is a member of the IEICE, Japan, and a senior member of IEEE. He was the recipient of the Young Engineer Award of the IEICE, the IEEE Antennas and Propagation Society (AP-S) Japan Chapter Young Engineer Award in 2004, the IEEJ Excellent Presentation Award, and the IEEE MTT-S Japan Young Engineer Award in 2011.

Toru Taniguchi was born in Tokyo, Japan, on December 6, 1956. He received the B.S. degree in Physics from the Nihon University, Tokyo, Japan, in 1981. From 1981 to 1992 he worked at 3rd. engineering section of Japan Radio Co. Ltd., and was engaged in development of microwave radio relay system. From 1993 to 2002 he worked at Saitama Laboratory of Japan Radio Co. Ltd., and engaged in research of high speed GaAs MESFET by ion implanting technology with Rapid Thermal Annealing. And from 2002 he is working at Laboratory of Japan Radio Co, LTD., and is currently engaging in research of mm wave Broad band wireless communication system. His main interests have been high frequency range broadband propagation and advanced modulation technology. Latest interest includes the design of ultra-compact high-reliability millimeter-wave broadband radio system with advanced modulation scheme.

Jiro Hirokawa was born in Tokyo, Japan, on May 8, 1965. He received the B.S., M.S. and D.E. degrees in electrical and electronic engineering from Tokyo Institute of Technology (Tokyo Tech), Tokyo, Japan in 1988, 1990 and 1994, respectively. He was a Research Associate from 1990 to 1996, and is currently an Associate Professor at Tokyo Tech. From 1994 to 1995, he was with the antenna group of Chalmers University of Technology, Gothenburg, Sweden, as a Postdoctoral Fellow. His research area has been in slotted waveguide array antennas and millimeter-wave antennas. Dr. Hirokawa received an IEEE AP-S Tokyo Chapter Young Engineer Award in 1991, a Young Engineer Award from IEICE in 1996, a Tokyo Tech Award for Challenging Research in 2003, a Young Scientists' Prize from the Minister of Education, Cultures, Sports, Science and Technology in Japan in 2005, a Best Paper Award in 2007, a Best Letter Award in 2009 from IEICE Communications Society and Asia Pacific Mirowave Conference prize in 2011. He is a fellow of IEEE.

Makoto Ando received the D.E. degree in electrical engineering from the Tokyo Institute of Technology, Tokyo, Japan, in 1979. From 1979 to 1983, he worked at Yokosuka Electrical Communication Laboratory, NTT, and was engaged in the development of antennas for satellite communication. He moved to Tokyo Institute of Technology in 1983 and is currently a Professor. His main interests have been high-frequency diffraction theory such as physical optics and geometrical theory of diffraction. His research also covers the design of reflector antennas, waveguide planar arrays and millimeter-wave antennas. Most recently, his interests include the design of high-gain millimeter-wave antennas and their systems. He received the Achievement Award and the Paper Awards from the IEICE Japan in 1993 and 2009. He was the general chair of the 2004 URSI EMT symposium in Pisa and of the ISAP 2007 in Niigata. He served as the member of the Scientific Council for the Antenna Centre of Excellence - ACE in the European Union's Sixth Framework Program from 2004 to 2007. He was the President of the Electronics Society of the IEICE in 2006 and the 2009 President of the IEEE Antennas and Propagation Society. He is a Fellow of the IEEE.